Global Change Biology **WILEY**

TECHNICAL ADVANCE

A field incubation approach to evaluate the depth dependence of soil biogeochemical responses to climate change

Xiaowei Guo[1] | Xiali Mao[1] | Wu Yu[1,2] | Liujun Xiao[1] | Mingming Wang[1] |
Shuai Zhang[1] | Jinyang Zheng[1] | Hangxin Zhou[1] | Lun Luo[3] |
Jinfeng Chang[1,4,5] | Zhou Shi[1,4,5] | Zhongkui Luo[1,4,5]

[1]College of Environmental and Resource
Sciences, Zhejiang University, Hangzhou,
China

[2]College of Resources and Environment,
Tibet Agricultural and Animal Husbandry
University, Nyingchi, China

[3]South-East Tibetan Plateau Station for
Integrated Observation and Research of
Alpine Environment, Institute of Tibetan
Plateau Research, Chinese Academy of
Sciences, Nyingchi, China

[4]Academy of Ecological Civilization,
Zhejiang University, Hangzhou, China

[5]Key Laboratory of Environment
Remediation and Ecological Health,
Ministry of Education, Zhejiang University,
Hangzhou, China

Correspondence
Zhongkui Luo, College of Environmental
and Resource Sciences, Zhejiang
University, Hangzhou 310058, China.
Email: luozk@zju.edu.cn

Abstract

Soil biogeochemical processes may present depth-dependent responses to climate change, due to vertical environmental gradients (e.g., thermal and moisture regimes, and the quantity and quality of soil organic matter) along soil profile. However, it is a grand challenge to distinguish such depth dependence under field conditions. Here we present an innovative, cost-effective and simple approach of field incubation of intact soil cores to explore such depth dependence. The approach adopts field incubation of two sets of intact soil cores: one incubated right-side up (i.e., non-inverted), and another upside down (i.e., inverted). This inversion keeps soil intact but changes the depth of the soil layer of same depth origin. Combining reciprocal translocation experiments to generate natural climate shift, we applied this incubation approach along a 2200m elevational mountainous transect in southeast Tibetan Plateau. We measured soil respiration (Rs) from non-inverted and inverted cores of 1m deep, respectively, which were exchanged among and incubated at different elevations. The results indicated that Rs responds significantly ($p < .05$) to translocation-induced climate shifts, but this response is depth-independent. As the incubation proceeds, Rs from both non-inverted and inverted cores become more sensitive to climate shifts, indicating higher vulnerability of persistent soil organic matter (SOM) to climate change than labile components, if labile substrates are assumed to be depleted with the proceeding of incubation. These results show in situ evidence that whole-profile SOM mineralization is sensitive to climate change regardless of the depth location. Together with measurements of vertical physiochemical conditions, the inversion experiment can serve as an experimental platform to elucidate the depth dependence of the response of soil biogeochemical processes to climate change.

KEYWORDS
decomposition, depth dependency, soil nutrient cycling, soil organic matter, temperature sensitivity, whole-soil

1 | INTRODUCTION

Soil is the largest terrestrial reservoir of organic matter (Friedlingstein et al., 2020), two-thirds of which store in the soil below 0.2 m

(Batjes, 2014; Jobbágy & Jackson, 2000). The turnover of this organic matter pool (the rate at which it enters and leaves the soil) regulates soil fertility, plant growth, and the climate. In an era of fighting against climate change, given the central role of soil organic matter (SOM)

dynamics in connecting the exchanges of elements between terrestrial and atmospheric pools, advanced understanding of whether and how whole-soil SOM cycling responds to climate change is vital for sustainable land management and effective climate actions. Soil biogeochemical cycling occurs in a three-dimensional, heterogeneous environment. It is crucial to distinguish potential depth-specific response of soil biogeochemical processes to climate change due to vertical environmental gradients (e.g., soil hydrothermal regimes, oxygen and substrate availability) through soil profile, and to elucidate underlying mechanisms.

Apparent vertical gradients exist through soil profile in terms of soil physical (e.g., thermal and moisture regimes), chemical (e.g., soil nutrient availability), and biological properties (e.g., microbial functionality and activity). As such, different controls/mechanisms may be involved in SOM turnover and persistence across soil depths (Lehmann & Kleber, 2015; Schmidt et al., 2011). For example, subsoil SOM has been found to be more persistent to decomposition than topsoil SOM due to greater aggregate protection and mineral adsorption than topsoil SOM (Qin et al., 2019). One of the suggested reasons is that topsoil SOM is dominated by substrates derived from plant materials, while most subsoil SOM is originated from microbial necromass which is more strongly protected against mineralization (Ni et al., 2020). In addition, both microbial community and soil organo-mineral interactions present vertical gradients through soil profile (Rumpel & Kögel-Knabner, 2011). These differences in SOM composition and protection processes across depths may result in distinct responses of SOM decomposition to climate change (Davidson & Janssens, 2006).

Depth-resolved assessment on soil biogeochemical processes as impacted by climate change is usually conducted in ideal laboratory conditions under artificial climate. For the elemental cycling of soil carbon, for example, with increasing soil depth, decreased, neutral, and increased temperature sensitivity had been found depending on soil and incubation conditions (Li et al., 2020; Qin et al., 2019; Vaughn & Torn, 2019). A reason for this inconsistence would be that such incubations are usually destructive, destroying micro-environmental gradient along soil profile and physiochemical protections of SOM. Field warming experiments provide a complementary, and have an advantage of reducing soil disturbance. Nevertheless, only few studies extend warming to deep whole-soil profile and assess depth-specific biogeochemical cycling (Hicks Pries et al., 2017). In addition, most existing field experiments with climate change treatments only focus on one or several climate variables (e.g., mean annual temperature and precipitation), ignoring that real climate change is an integrated phenomenon of changes of various climate variables such as the frequency and intensity of climate extremes. It is also very expensive to set up and maintain this kind of field manipulative experiments. Overall, we need novel approaches/technologies to conduct in situ depth-resolved quantification of soil biogeochemical responses to climate change, and overcome the challenges of intact sampling and/or monitoring in soil depths (Maier & Schack-Kirchner, 2014).

Here we propose an innovative approach of field incubation of intact soil cores to explore the depth dependence of the responses of soil biogeochemical processes to climate change. This approach was illustrated in a 2200 m elevational transect in southeast Tibetan Plateau to test two topical hypotheses relating to whole-soil biogeochemical cycles. That is, depth-associated soil profile environmental gradients influence not only soil carbon mineralization (H1) but also its sensitivity to climate change (H2). The approach can be applied to address other questions by measuring variables of interest, designing incubation treatments, or conducting additional experiments using soil samples harvested from the incubated soil cores.

2 | MATERIALS AND METHODS

2.1 | The field incubation approach

The approach relies on natural climate shifts across sites to generate a natural climate gradient. Intact soil cores are extracted at sites with different climate, and then reciprocally translocated (i.e., exchanged among sites) and incubated at the sites under different ambient climatic condition. This design has been adopted to study the response of soil biogeochemical responses to climate change (Hu et al., 2016; Ni et al., 2021; Nottingham et al., 2019; Zimmermann et al., 2009).

Together with the reciprocal translocation, a soil core inversion treatment is designed to change the depth location of soil layer of same depth origin (Figure 1). That is, the sampled soil cores are divided into two groups: one group is incubated right-side up (i.e., non-inverted), and another upside down (i.e., inverted). This inversion keeps soil core intact but, depending on the choice of the depth of soil cores, creates contrasting environmental conditions for the soil layer of same depth origin, enabling in situ assessment of the depth dependence of soil biogeochemical processes as well as their responses to climate change. Figure 1 diagrams this approach using an elevational transect to generate climate shifts. The approach can be applied to any climate transects if logistics is not an issue, and the inversion treatment can be also combined with other treatments of global change factors (e.g., manipulation of carbon/nutrient input and soil disturbance) to evaluate other questions relating to soil biogeochemical cycle-global change feedbacks.

Here we summarize some vertical gradients which could be altered by the inversion treatment (Figure 2):

1. *Soil hydrothermal regimes*. Soil moisture and thermal environment are more stable in deeper depths. The inversion would reverse the hydrothermal fluctuations in the original surface and bottom soil layers. In addition, topsoil usually has higher SOM content than subsoil. As SOM-rich soils have higher porosity and water holding capacity, the inversion change the vertical profile of soil moisture dynamics. Since air and water share the pore space of soil, changes in moisture regime would also alter O_2 availability through soil profile.

2. *O_2 availability*. There is a higher probability of higher O_2 availability in topsoil than in subsoil (Ebrahimi & Or, 2016). Most biogeochemically active elements concentrate in the surface layer where O_2 is not or less limited. When this original surface layer is flipped down to deeper depths, O_2—as a critical and strong

FIGURE 1 An example to demonstrate the field incubation experiment. Soil cores from three elevations are reciprocally translocated and incubated in ambient climatic condition. This design allows in situ quantification of soil biogeochemical processes in response to climate change induced by elevation shift. Together with the translocation, a soil core inversion treatment is designed to change the depth location of soil of the same depth origin, enabling in situ assessment of the depth dependence of soil biogeochemical responses to climate change. [Colour figure can be viewed at wileyonlinelibrary.com]
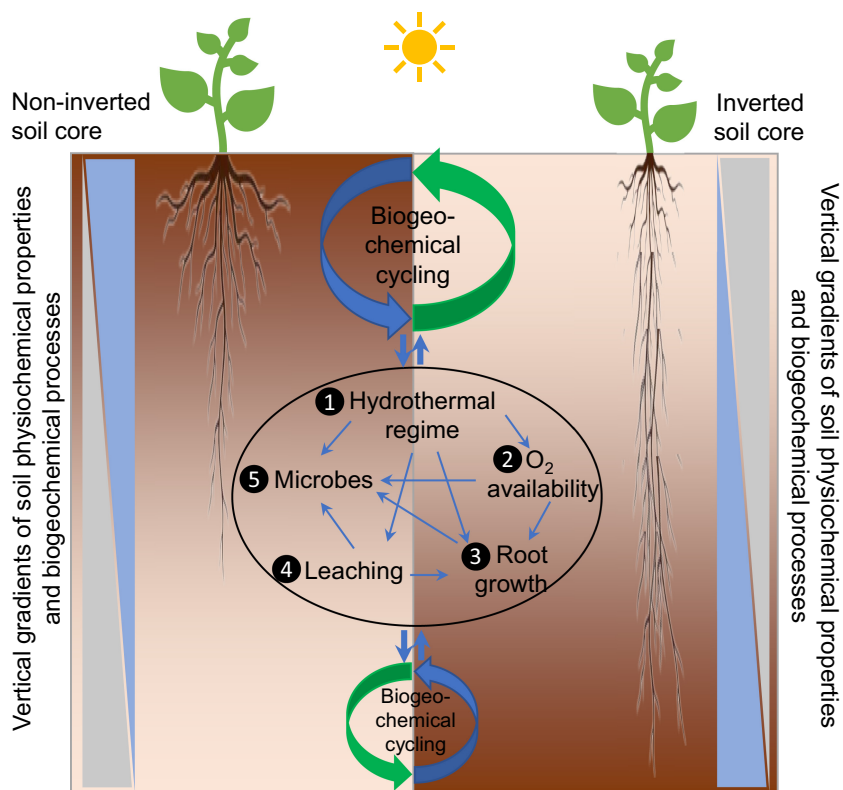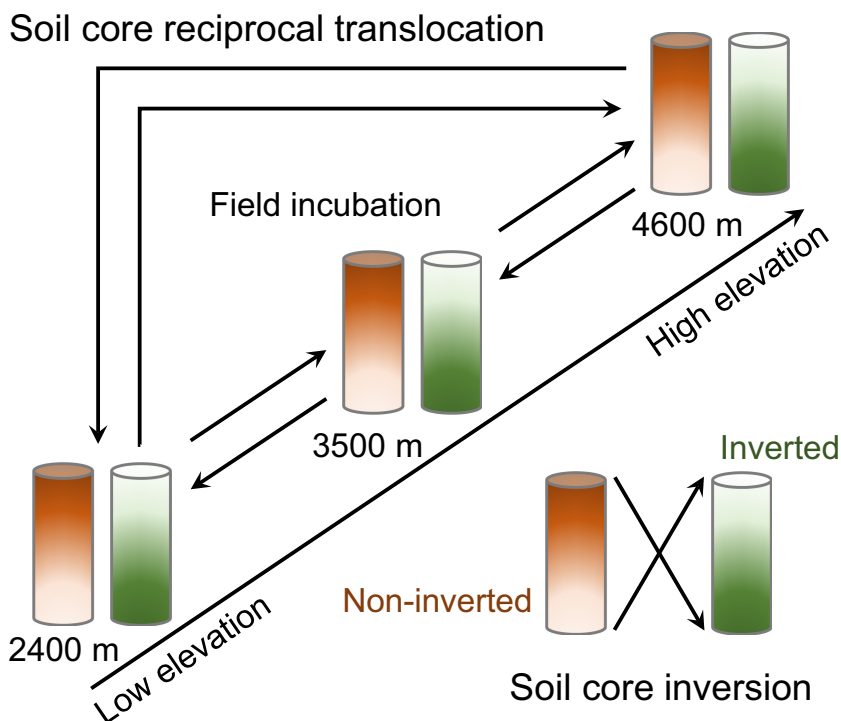
FIGURE 2 A schematic diagram shows the effects of inversion on vertical gradients of soil environment and processes. This inversion places the soil of the same depth origin into different soil depths, resulting in changes in, but not limited to, soil moisture and thermal regimes (①), O_2 availability (②), root growth (e.g., the depth distribution of root biomass, ③), the quantity and quality of vertically transported soil organic matter and nutrients (④), and microbial community composition, activity, and functionality (⑤). The blue and gray triangles on the left illustrate two types (i.e., decrease vs. increase with soil depth, respectively) of vertical gradients of soil physiochemical properties and biogeochemical processes in non-inverted soil cores. The gradient pattern is inverted in inverted soil cores as shown on the right. The inversion treatment provides a convenient way to explore how these processes and their interconnections control soil biogeochemical processes. [Colour figure can be viewed at wileyonlinelibrary.com]

oxidizing agent in upland soils—would become deficit or limited because of increased requirement for SOM oxidization, root respiration (see the discussion below on *Plant root growth*) as well as oxidation–reduction of elements.

3. *Substrate vertical movement*. Another important gradient change relates to the movement of substrates (e.g., dissolved carbon) and nutrients (e.g., active nitrogen) driven by vertical water flow through soil profile (Ahrens et al., 2015). The direction of those movements will be reversed by the inversion treatment. When deep soil is lifted to the surface, for example, it will loss rather than receive dissolved carbon and nutrients. This may substantially change the interactions between SOM pools via such as the priming effect (Luo et al., 2020).

4. *Plant root growth*. If plant growth is permitted in the incubated cores, plants would allocate more carbon into deeper depths in inverted cores to acquire water and nutrients therein as the SOM and nutrient-rich surface soil layer has been flipped down. This change of the depth allocation of belowground carbon can help understand how carbon storage in different soil depths associates with carbon inputs therein, and assess carbon pool interactions under different environmental conditions.

5. *Microbial community shift*. Microbial community composition, function and activity present a vertical gradient due to the close association of microbial physiological and metabolic properties with edaphic properties. For example, inversion would induce changes in carbon inputs in terms of both quantity and quality to the soil layer of same depth origin via processes discussed above, and thus results in shifts in microbial composition, activity, metabolism and interspecific relationships (Sokol et al., 2022).

Depending on soil properties such as texture and physical structure (e.g., aggregates), these vertical gradients may vary substantially among soils. The inversion treatment provides a good opportunity to test whether and how various processes regulate whole-soil biogeochemical processes, accompanying with depth-specific measurements and long-term monitoring. Especially, we suggest that soil cores can be harvested after a period of incubation. These harvested soils can be separated into layers of same depth origin with the measurement of biological and physicochemical properties, and then compared between inverted and non-inverted cores. The harvested soils also provide an excellent source for laboratory incubation to address how changes in carbon pool composition and microbial community and their interactions influence the response of soil biogeochemical processes to treatments of global change factors (e.g., warming, substrate quantity and quality, nutrient addition).

2.2 | Statistical metrics for assessing the effects of soil core inversion

We suggest a simple metric to test hypotheses relating to whether and how depth-induced environmental gradients influence soil biogeochemical processes (H1). For a typical variable (V), a log response ratio (RR) using V measured for the soil layer of same depth origin from inverted and non-inverted cores incubated at the same site can be calculated as:

$$RR_{H1} = \ln\left(\frac{V_i^*}{V_i}\right), \tag{1}$$

where V_i^* and V_i are the measurements of a typical variable in the ith soil layer from inverted and non-inverted soil cores, respectively.

To test hypotheses relating to how depth-induced environmental gradients influence the response of V to climate shifts (or other global change factors, H2), the log response ratio for inverted and non-inverted cores can be calculated, respectively, as:

$$RR_{H2} = \ln\left(\frac{V_{i,dest}}{V_{i,orig}}\right), \tag{2}$$

$$RR_{H2}^* = \ln\left(\frac{V_{i,dest}^*}{V_{i,orig}^*}\right), \tag{3}$$

where $V_{i,dest}$ and $V_{i,orig}$ are the V_i from non-inverted soil cores translocated to other climate destination and reinstalled at the origin climate, respectively; $V_{i,dest}^*$ and $V_{i,orig}^*$ are the V_i from inverted soil cores translocated to other climate destinations and reinstalled at the origin climate, respectively. Then, RR_{H2} and RR_{H2}^* can be statistically compared. Regression analyses can also be conducted to assess the relationship of RR_{H1}, RR_{H2} and RR_{H2}^* with climate shifts. If different soils have been treated, regression analyses can also be used to assess how soil physiochemical properties impact the response.

2.3 | Case study sites

To demonstrate the field incubation approach, three sites were selected along a 2200m elevational transect ranging from 2400 to 4600m at Mount Segrila in southeast Tibet. The elevations of the three sites are ~2400, ~3500, and ~4600m with a mean annual temperature of 11.1, 3.4, and −1.3°C, respectively, and mean annual precipitation of 844, 985, and 1057mm, respectively. The soil is a dark-brown Cambisols. The 4600m site is a natural alpine meadow with *Polygonum macrophyllum* D. Don, *Rhodiola fastigiate* S.H. Fu and *Potentilla peduncularis* D. Don as the dominant plant species. The 3500m site is a grazed pasture dominated by *Iris bulleyana* Dykes, *Veronica polita* Fries, *Primula alpicola* Stapf and *Carex haematostoma* Nees. The 2400m site is an alpine barley cropland with a long history of cultivation. The different land use has an advantage of testing the importance of soil heterogeneity. More detailed descriptions of the study sites and soil properties have been presented in Table 1.

2.4 | Soil sampling and measurements

In early September 2020, at each site, soil samples with five replicates ($n = 5$) from five depth intervals/layers (i.e., 0–10, 10–20, 20–30, 30–50, and 50–100cm) were extracted and sieved to 2mm to remove stones and roots and divided into two subsamples: one was

TABLE 1 Depth-specific soil properties (mean ± SE, $n = 5$)

Elevation	Variable	0–10 cm	10–20 cm	20–30 cm	30–50 cm	50–100 cm
2400 m	pH	6.26 ± 0.01	6.36 ± 0.01	6.58 ± 0.01	6.66 ± 0.02	6.68 ± 0.01
	Total nitrogen (%)	0.131 ± 0.002	0.098 ± 0.004	0.068 ± 0.002	0.052 ± 0.003	0.034 ± 0.003
	Carbon:nitrogen	10.93 ± 0.11	10.76 ± 0.04	10.63 ± 0.22	9.87 ± 0.14	15.63 ± 0.77
	NH_4^+-N (mg kg^{-1})	1.11 ± .03	0.90 ± 0.16	0.83 ± 0.16	0.69 ± 0.13	0.56 ± .11
	NO_3^--N (mg kg^{-1})	1.53 ± 0.16	1.60 ± 0.20	0.98 ± 0.22	0.26 ± 0.09	0.10 ± 0.03
	DOC (mg kg^{-1})	184.89 ± 12.4	119.96 ± 17.3	84.49 ± 18.8	54.71 ± 6.23	39.19 ± 4.51
	DON (mg kg^{-1})	7.80 ± 1.13	6.83 ± 0.86	5.43 ± 0.23	5.69 ± 0.39	5.25 ± 0.34
	POC (g kg^{-1})	29.60 ± 3.43	9.08 ± 1.66	3.133 ± 0.62	1.65 ± 0.42	1.40 ± 0.66
	MOC (g kg^{-1})	27.00 ± 3.21	18.99 ± 0.99	8.50 ± 1.64	5.04 ± 0.90	2.93 ± 0.71
	Fe and Al Oxides_d (mg kg^{-1})	7.43 ± 0.02	6.93 ± 0.09	6.85 ± 0.05	5.94 ± 0.10	5.18 ± 0.21
	Fe and Al Oxides_o (mg kg^{-1})	2.86 ± 0.33	1.01 ± 0.03	1.14 ± 0.05	1.18 ± 0.07	1.50 ± 0.12
	Silt (%)	22.92 ± 0.25	23.12 ± 2.20	22.22 ± 1.23	20.99 ± 2.08	24.82 ± 1.63
	Clay (%)	2.70 ± 0.16	2.80 ± 0.28	2.74 ± 0.21	2.46 ± 0.18	3.06 ± 0.45
	Bulk density (g m^{-3})	0.83 ± 0.03	0.93 ± 0.03	0.98 ± 0.04	1.18	1.29
	MBC (mg kg^{-1})	383.97 ± 13.9	292.16 ± 16.4	193.13 ± 13.3	142.50 ± 2.9	98.30 ± 0.88
	MBC:MBN	6.11 ± 0.06	5.68 ± 0.11	6.34 ± 0.06	4.44 ± 0.02	4.25 ± 0.06
	Fungi (nmol g^{-1})	1.09 ± 0.05	—	—	—	0.21 ± 0.01
	Bacteria (nmol g^{-1})	11.42 ± 0.56	—	—	—	3.61 ± 0.17
	Aerobes (nmol g^{-1})	1.88 ± 0.11	—	—	—	0.31 ± 0.02
	Anaerobes (nmol g^{-1})	0.71 ± 0.04	—	—	—	0.11 ± 0.01
	Aerobes:anaerobes	2.66 ± 0.01	—	—	—	2.81 ± 0.13
3500 m	pH	6.02 ± 0.03	5.97 ± 0.04	5.91 ± 0.01	5.95 ± 0.05	6.54 ± 0.01
	Total nitrogen (%)	0.471 ± 0.006	0.262 ± 0.010	0.134 ± 0.007	0.073 ± 0.004	0.022 ± 0.001
	Carbon:nitrogen	11.40 ± 0.06	11.93 ± 0.24	16.81 ± 0.72	14.29 ± 0.68	13.39 ± 0.84
	NH_4^+-N (mg kg^{-1})	2.04 ± 0.11	1.65 ± 0.12	1.75 ± 0.10	1.49 ± .23	0.77 ± 0.08
	NO_3^--N (mg kg^{-1})	2.39 ± 0.21	2.16 ± 0.16	1.74 ± 0.29	0.63 ± 0.12	0.08 ± 0.03
	DOC (mg kg^{-1})	229.40 ± 20.9	93.44 ± 12.8	32.46 ± 7.14	19.14 ± 3.08	10.85 ± 0.85
	DON (mg kg^{-1})	12.64 ± 1.48	7.38 ± 0.07	5.20 ± 1.18	2.99 ± 0.61	1.97 ± 0.22
	POC (g kg^{-1})	58.68 ± 10.97	22.21 ± 1.30	13.23 ± 1.55	7.28 ± 0.98	2.35 ± 0.34
	MOC (g kg^{-1})	20.48 ± 1.39	19.86 ± 0.27	13.80 ± 1.22	7.90 ± 0.67	3.64 ± 0.08
	Fe and Al Oxides_d (mg kg^{-1})	26.83 ± 0.19	34.0 ± 0.21	32.57 ± 0.30	22.33 ± 0.18	16.22 ± 0.58
	Fe and Al Oxides_o (mg kg^{-1})	6.40 ± 0.09	8.03 ± 0.06	7.00 ± 0.30	4.43 ± 0.35	1.61 ± 0.11
	Silt (%)	59.62 ± 6.41	50.56 ± 14.86	62.02 ± 8.88	43.47 ± 13.34	37.92 ± 5.06
	Clay (%)	4.86 ± 0.63	4.11 ± 1.04	6.53 ± 0.45	6.12 ± 1.62	6.68 ± 0.37
	Bulk density (g m^{-3})	0.93 ± 0.01	1.03 ± 0.02	1.01 ± 0.03	1.43 ± 0.03	1.56
	MBC (mg kg^{-1})	920.97 ± 9.96	532.78 ± 5.32	372.65 ± 2.58	219.22 ± 1.09	96.54 ± 5.72
	MBC:MBN	11.8 ± 0.10	9.68 ± 0.16	8.28 ± 0.14	6.56 ± 0.04	4.84 ± 0.19
	Fungi (nmol g^{-1})	3.20 ± 0.60	—	—	—	0.35 ± 0.20
	Bacteria (nmol g^{-1})	24.31 ± 4.20	—	—	—	4.08 ± 1.61
	Aerobes (nmol g^{-1})	5.12 ± 3.15	—	—	—	0.47 ± 0.33
	Anaerobes (nmol g^{-1})	2.15 ± 0.45	—	—	—	0.19 ± 0.16
	Aerobes:anaerobes	2.39 ± 0.02	—	—	—	2.18 ± 0.001

(Continues)

TABLE 1 (Continued)

Elevation	Variable	0–10 cm	10–20 cm	20–30 cm	30–50 cm	50–100 cm
4600 m	pH	5.15 ± 0.01	5.30 ± 0.02	5.40 ± 0.02	5.42 ± 0.09	5.58 ± 0.01
	Total nitrogen (%)	0.369 ± 0.005	0.271 ± 0.003	0.164 ± 0.018	0.074 ± 0.010	0.039 ± 0.000
	Carbon:nitrogen	14.22 ± 0.06	15.07 ± 0.14	13.64 ± 0.79	9.87 ± 0.95	13.47 ± 0.31
	NH_4^+-N (mg kg^{-1})	4.68 ± 0.32	4.85 ± 0.63	3.33 ± 0.43	$2.39 \pm .33$	1.38 ± 0.18
	NO_3^--N (mg kg^{-1})	3.01 ± 0.34	1.95 ± 0.28	1.26 ± 0.32	0.66 ± 0.10	0.44 ± 0.02
	DOC (mg kg^{-1})	72.52 ± 4.72	43.40 ± 6.46	29.50 ± 9.71	18.64 ± 3.90	8.27 ± 1.74
	DON (mg kg^{-1})	16.62 ± 2.23	9.79 ± 1.63	6.93 ± 2.30	6.67 ± 0.66	5.63 ± 1.26
	POC (g kg^{-1})	45.49 ± 7.38	24.54 ± 3.40	13.61 ± 0.02	7.97 ± 1.34	4.18 ± 1.83
	MOC (g kg^{-1})	21.87 ± 0.71	15.16 ± 2.72	13.30 ± 1.82	9.33 ± 1.11	6.06 ± 1.39
	Fe and Al Oxides_d (mg kg^{-1})	26.77 ± 0.04	33.32 ± 0.32	31.76 ± 0.28	28.02 ± 0.12	24.19 ± 0.39
	Fe and Al Oxides_o (mg kg^{-1})	10.1 ± 0.32	13.07 ± 0.64	12.99 ± 0.87	8.84 ± 0.66	6.86 ± 0.17
	Silt (%)	44.92 ± 4.77	59.29 ± 8.49	52.42 ± 4.58	48.90 ± 4.44	37.85 ± 10.14
	Clay (%)	5.48 ± 0.56	4.86 ± 0.75	5.03 ± 0.79	4.93 ± 0.52	4.64 ± 0.41
	Bulk density (g m^{-3})	1.44 ± 0.11	1.48 ± 0.06	1.50 ± 0.16	1.47 ± 0.03	1.48
	MBC (mg kg^{-1})	1020.2 ± 29.5	656.46 ± 21.7	345.8 ± 11.07	207.9 ± 12.41	179.82 ± 2.41
	MBC:MBN	9.35 ± 0.01	9.18 ± 0.02	6.87 ± 0.14	6.09 ± 0.00	6.78 ± 0.04
	Fungi (nmol g^{-1})	2.30 ± 0.10	—	—	—	0.12 ± 0.01
	Bacteria (nmol g^{-1})	18.86 ± 0.56	—	—	—	1.94 ± 0.19
	Aerobes (nmol g^{-1})	3.70 ± 0.14	—	—	—	0.08 ± 0.01
	Anaerobes (nmol g^{-1})	1.84 ± 0.04	—	—	—	0.02 ± 0.01
	Aerobes:anaerobes	2.01 ± 0.03	—	—	—	3.79 ± 0.87

Note: DOC and DON are the dissolved organic carbon and nitrogen, respectively; POC and MOC are the particulate and mineral-associated organic carbon, respectively; Oxides_d and Oxides_o are the free and amorphous Fe and Al oxides, respectively; MBC and MBN are the microbial biomass carbon and nitrogen, respectively.

air-dried for determining soil physicochemical properties, and the other was stored at −20°C for later measurement of inorganic nitrogen (NH_4^+-N and NO_3^--N) and microbial properties. At the time of soil sampling, temperature data loggers (iButton; model DS1921G, Dallas Semiconductor, TX, USA) were placed in the middle depth of each layer to automatically monitor and record soil temperature every 4 h for 1 year at the sampling sites (Figure 3).

Using the air-dried samples, soil organic C and total nitrogen (N) were analysed using an elemental analyser (Elementar, Germany). Dissolved organic C and N was determined by measuring C and N concentration in the $0.5 \, mol \, L^{-1} \, K_2SO_4$ extract solution (soil: solution = 1:4) after filtering through a membrane filter with 0.45-μm pores using Multi 3100 N/C TOC analyser (Analytik Jena, Germany). Soil pH was measured using a pH electrode (soil-water suspension in a 1:2.5 (w: v), Mettler-161 Toledo, Switzerland). Soil texture was determined using a laser particle size analyser (LS-CWM, OMEC, China). Particulate (POC) and mineral-associated organic carbon (MOC) were determined using soil samples fractionated by size (53 μm) after full soil dispersion following the procedure described by Cotrufo et al. (2019). The free oxides (i.e., Fe_d, Al_d) and amorphous oxides (Fe_o, Al_o) were extracted with dithionite-citrate-bicarbonate solution and ammonium-oxalate solution, respectively, and then analyzed by inductively coupled plasma optical

emission spectroscopy (Optima 2000, PerkinElmer Co.). Chemical composition of soil organic C was determined via ^{13}C CPMAS NMR in solid-state (AVANCE NEO 600 MHz, Bruker-Biospin, Switzerland). The recorded ^{13}C spectra were quantified in the following chemical shift regions: alkyl C (0–45 ppm), O-alkyl C (45–110 ppm), aromatic C (110–160 ppm), and carbonyl/carboxyl C (160–220 ppm). The ratio of alkyl C to O-alkyl C was calculated to describe the degree of C decomposition, the ratio of hydrophobic (alkyl C + aromatic C) to hydrophilic C (O-alkyl C + carbonyl/carboxyl C) to describe soil C stability due to aggregation protection, and the ratio of aromatic C to the sum of C in the region of 0–160 ppm to describe the complexity of organic molecular structure (Baldock et al., 1997). We should note that, due to the high cost of ^{13}C CPMAS NMR, the five replicates were mixed to a composite sample (i.e., no replicates) for the measurement of chemical composition.

Using fresh samples, NH_4^+-N and NO_3^--N were analysed calorimetrically by a continuous flow analyser (SEAL AA3, Norderstedt, Germany). Microbial biomass C and N (i.e., MBC and MBN) were measured using the fumigation extraction method (Vance et al., 1987). MBC and MBN were calculated as the difference in extractable C and N before and after fumigation using a conversion factor of 0.45 and 0.54, respectively. Microbial community structure was assessed by analysing the composition of extractable
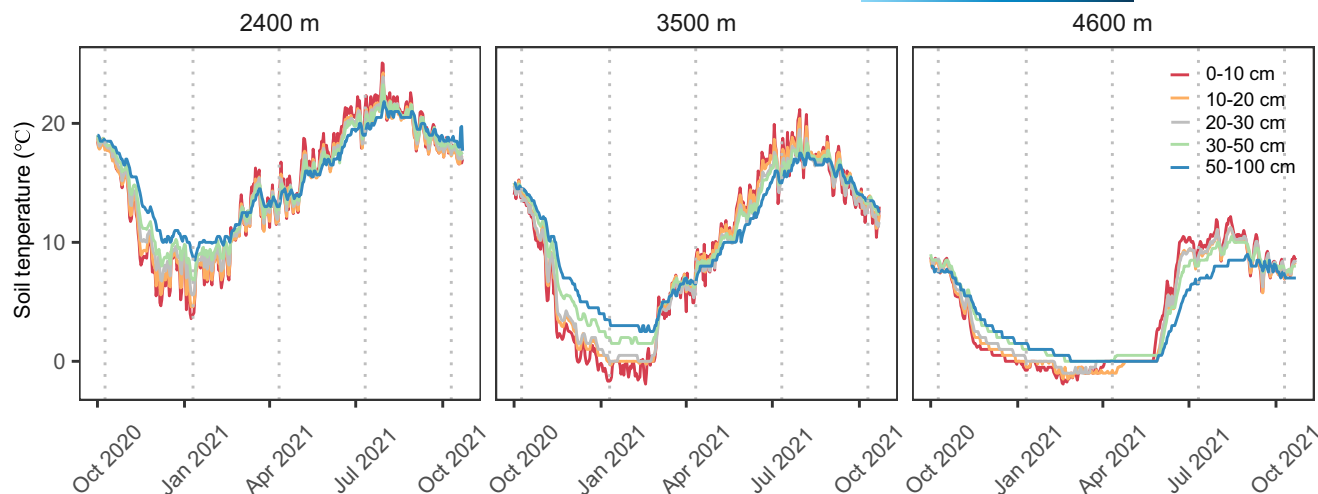
FIGURE 3 Soil temperature records in different depths of the nearby soil of incubated cores at three elevations. [Colour figure can be viewed at wileyonlinelibrary.com]

ester-linked phospholipid fatty acids (PLFAs) (Bossio & Scow, 1998). Concentrations of individual PLFAs were calculated based on 19:0 internal standard concentrations. PLFAs indicators were used to classify microbial functional types. Fungi community was represented by PLFAs 18:1ω9c, 18:2ω6c, 18:3ω6c; bacterial community was represented by PLFAs 14:0, a14:0, i14:0, 15:0, a15:0, i15:0, 16:0, a16:0, i16:0, 17:0, a17:0, i17:0, 18:0, i18:0, i19:0, 14:1ω5c, 14:1ω9c, 15:1ω5c, 15:1ω7c, 15:4ω3c, 16:1ω5c, 16:1ω7c, 16:1ω9c, 16:3ω6c, cy17:0, 17:1ω8c, 18:1ω5c, 18:1ω7c, cy19:0, 19:1ω8c, and 19:3ω6c. Aerobic bacteria were also identified using PLFAs 16:1ω7c and 18:1ω9c; and anaerobic bacteria using PLFAs cy17:0 and cy19:0.

2.5 | Field incubation

At the time of soil sampling (September 2020), at each elevation, 60 cores (1 m deep) of intact mineral soil in the sampling quadrats were extracted over the complete 1 m soil profile using a mechanized auger (Rhino S1, USA), with an inside diameter of 3.7 cm of the PVC tubes. Twenty cores were retained at the same elevation, and the other 40 cores were translocated to other two elevations. At each elevation, half of the 20 cores from the same elevation (i.e., $n = 10$) were reinstalled at their original vertical direction (i.e., non-inverted); and the other half was reinstalled inversely (i.e., inverted, Figure 1).

The 1 m deep soil cores with the PVC tubes were incubated in the field under ambient climate condition. At the start of incubation, all plants and visible plant litter in all soil cores were removed. After 1 month of the reinstallation and allowing the incubated soil cores to stabilize, soil CO_2 efflux (Rs, μmol CO_2 m^{-2} s^{-1}) from the soil cores was measured at seasonal interval from October in 2020 to October in 2021 (i.e., a total of five measurements, except April 2021 at the 4600 m elevation due to storm and deep snow) using an automated soil chamber CO_2 flux system (LI-8100A, Li-Cor Inc.). As the diameter of the chamber (20 cm) is larger than the diameter of the incubated soil cores (3.7 cm), a plastic liner is used which only allows CO_2 efflux from the incubated cores go to the chamber. Visible

living plants and plant litter in the core were removed 1 day ahead of the CO_2 efflux measurements to limit plant autotrophic respiration. Measurements were made during 9:00 a.m. to 16:00 p.m. on each scheduled day (Figure 3).

2.6 | Statistical analyses

To test Hypothesis 1, that is, depth-induced environmental gradients influence soil respiration Rs, a log response ratio (RR_{H1}) was calculated using Equation (1). A non-parametric bootstrap approach of 200 bootstrapping samples was used to estimate RR_{H1} and its uncertainty. For each bootstrapping sample, 10 Rs^* and Rs values were randomly drawn from the 10 replicates of Rs measurements of inverted and non-inverted cores, respectively, with replacement. Then, based on the 200 bootstrapping estimates, the average of RR_{H1} was estimated and its 95% confidence intervals (CI) were calculated as their 2.5% and 97.5% quantiles. A one-sample bootstrap t-test (Efron & Tibshirani, 1993) was conducted to assess whether RR_{H1} is significantly different from 0 (i.e., soil core inversion has significant effect on Rs).

To test Hypothesis 2, that is, depth-induced environmental gradients influence the response of soil C decomposition to climate shifts, the log response ratio for inverted (RR_{H2}^*) and non-inverted cores (RR_{H2}) were calculated using equations (2) and (3), respectively. Similar to RR_{H1}, 200 bootstrapping estimates were used to estimate the mean and 95% CI for RR_{H2} and RR_{H2}^*. A two-sample bootstrap t-test was conducted to assess whether RR_{H2} and RR_{H2}^* are significantly different. A linear regression was also conducted to assess the relationship of RR_{H2} and RR_{H2}^* with elevation shifts. All calculations and statistical analyses were performed in R 4.0.3 (R Core Team, 2022).

3 | RESULTS AND DISCUSSION

The core of this study is to introduce the field incubation approach using a soil core inversion treatment. This approach non-destructively changes

the depth location of soil from the same depth origin, resulting in distinct environmental conditions for the soil of same depth origin (Figure 2). Together with translocation experiments among climate-distinct sites, it thus has the potential to separate depth location-induced effects of the responses of soil biogeochemical processes to climate shift. Here we report the results of the response of soil respiration as a case study, and discuss the limitations and potential implications.

3.1 | Vertical environmental gradients through soil profile

The three soils present an apparent gradient of soil texture, with less and greater clay content in deeper layers at 4600 and 3500 m elevations, respectively (Table 1). At 2400 m, clay content is generally similar across soil depths but only half of that at the 3500 and 4600 m elevations (Table 1). SOC content shows distinct depth distributions at the three elevations (Figure 4a). At two higher elevations, SOC content decreases with depth, ranging from 5.37 ± 0.09% (mean ± one standard error) in the 0–10 cm soil layer to 0.30 ± 0.01% in the 50–100 cm soil layer. At the 2400 m elevation, it is relatively constant across soil depths with an average of ~1% (Figure 4a). In terms of the chemical composition of SOC, the proportion of aryl C, the ratio of aryl to O-alkyl C and the ratio of hydrophobic to hydrophilic C increase with soil depth (Figure 4b–d). The aromaticity also varies across soil depths and elevations (Figure 4e). The proportion of MOC to total SOC increases from 47.5 ± 5.8, 26.9 ± 3.6 and 33.4 ± 4.4% in the 0–10 cm soil layer to 70.7 ± 4.9%, 61.1 ± 3.1% and 62.0 ± 4.7% in the 50–100 cm soil at the 2400, 3500 and 4600 m elevation, respectively (Table 1). The free (i.e., Fe_d and Al_d) and amorphous (i.e., Fe_o and Al_o) metal oxides decrease with depth and vary across the three elevations (Table 1). The soil microbial PLFAs (i.e., fungi, bacteria, aerobes and anaerobes) in the topsoil (0–10 cm) are significantly higher than that in the subsoil (50–100 cm, $p < .05$), and the ratios of aerobes to anaerobes in both topsoil and subsoil layers are greater than 2 at all three elevations (Table 1). Overall, these results demonstrate clear, but distinct, vertical gradients of SOC chemical composition, physiochemical protection and microbial activity through soil profiles at different sites.

3.2 | Soil core inversion-induced changes in soil respiration

Lower Rs was generally observed from inverted cores (i.e., negative RR_{H1} response), but this response was insignificant ($p > .05$) irrespective of elevation, climate shift, and measurement time (Figure 5a). This result does not support the expectation that respiration from inverted soil cores would be smaller than that from non-inverted cores, due to original surface layers (where are usually rich in both carbon substrates and other resources, Figure 4 and Table 1) are buried into deep depths where would suffer from more environmental constraints. Oxygen availability has been suggested to be a such
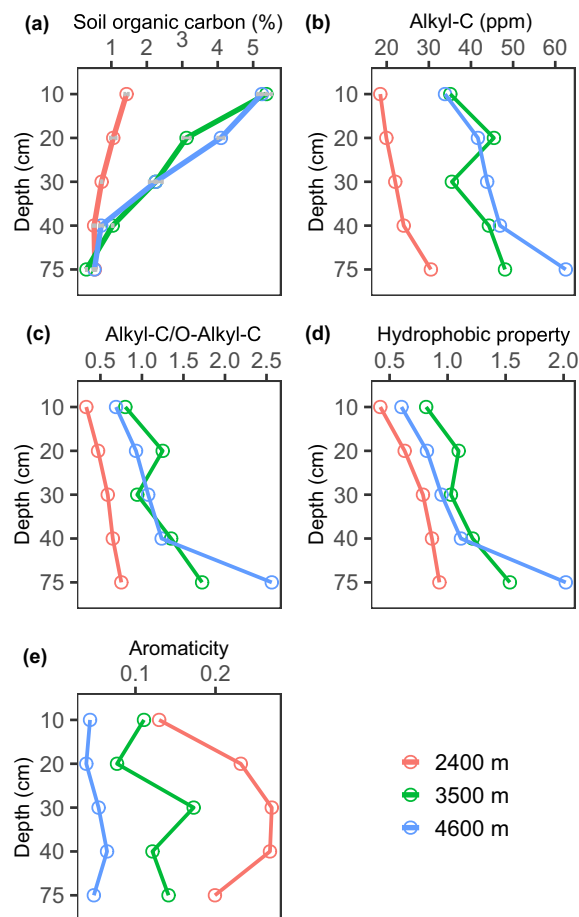

FIGURE 4 Selected chemical properties of soil organic carbon in different soil depths at three elevations. Hydrophilic property shows the ratio of the sum of alkyl C and aromatic C to the sum of O-alkyl C and carbonyl/carboxyl C; aromaticity is estimated as the ratio of aromatic C to the sum of C in the region of 0–160 ppm. Error bars in (a) show one standard error (mean ± SE, $n = 5$). For other properties showed in (b–e), one composite sample was measured due to high cost. [Colour figure can be viewed at wileyonlinelibrary.com]

constraint in subsoil which would take effect in short term. This result implies that O_2 is likely to be still sufficient for carbon decomposition even in the depth of 1 m. There are two reasons. First, if O_2 is limited in deeper depth, inverted soil cores would have much lower respiration than non-inverted cores as there are much more carbon in deeper depths in inverted soil cores (Figure 4a). Second, aerobic microbes are dominant in both topsoil and subsoil (i.e., 0–10 and 50–100 cm) at all three elevations (Table 1). There is also evidence that even O_2 level of 5% were sufficiently high for microbial decomposition (Salomé et al., 2010), and depth translocation has no or only minor effects on microbial biomass, community structure and activity (Preusser et al., 2017). A process-based modelling also showed that O_2 limitation on carbon decomposition was only occur when O_2 diffusion rates in deeper layers are reduced by 1000 to 10,000 times compared with the rate in topsoil (Kirschbaum et al., 2021).

In our case study, we did not measure O_2 availability. The insignificant response of soil respiration to the inversion treatment (Figure 5a) does not invalidate the possibility that there is a trade-off

FIGURE 5 Temporal response ratios of soil respiration to depth location (a) and elevation shifts (b). (a) The response ratios of soil carbon decomposition to changes in depth location induced by soil core inversion treatment under different elevation shifts (i.e., hypothesis 1). (b) The response ratios of soil carbon decomposition in inverted (green symbols) and non-inverted (brown symbols) cores to elevation shifts (i.e., hypothesis 2). Lines are regression lines for non-inverted and inverted cores, respectively, with the color legends show the corresponding regression slopes. Error bars show 95% confidence intervals. [Colour figure can be viewed at wileyonlinelibrary.com]
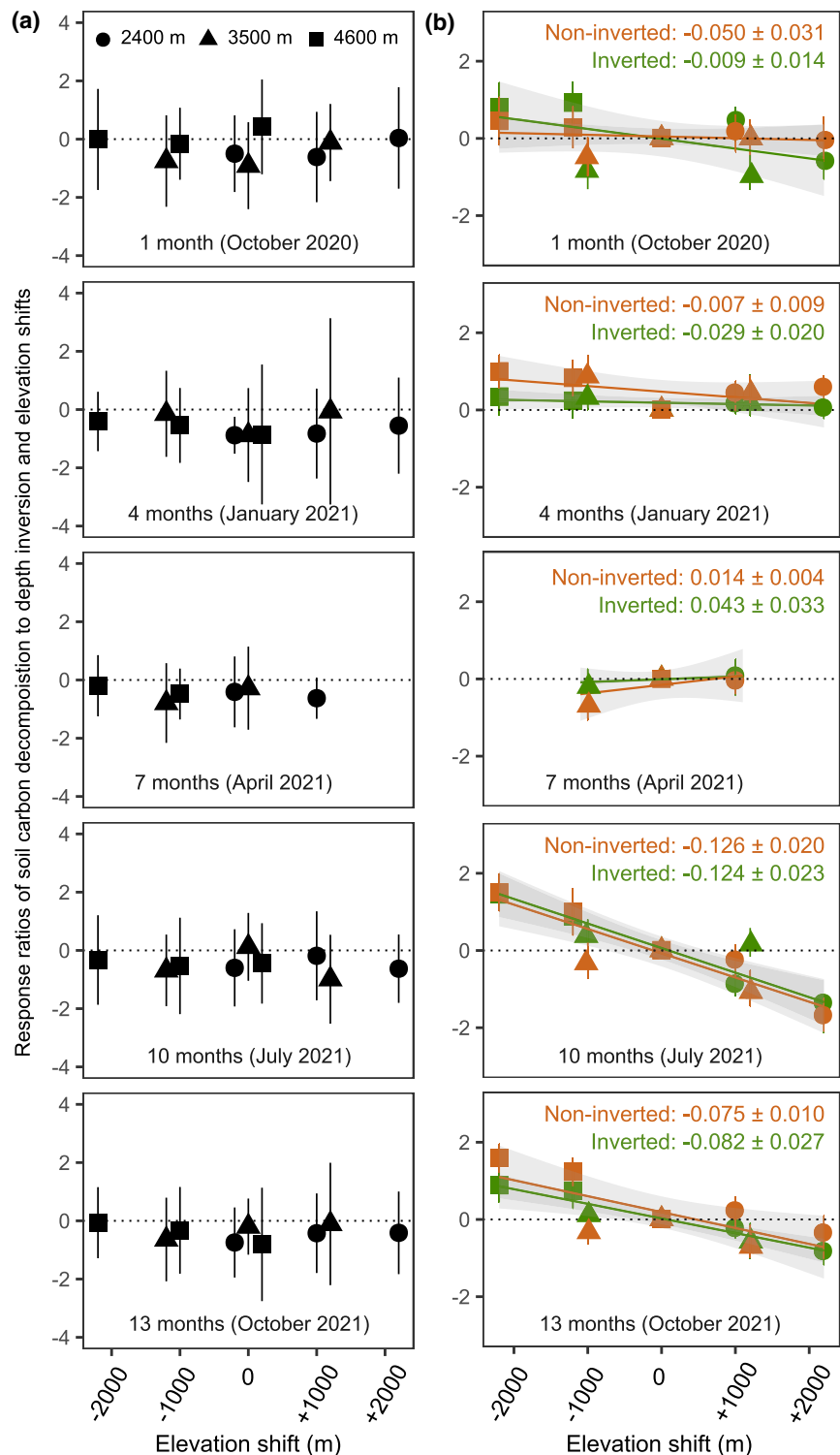
between physicochemical and kinetic/thermodynamic carbon protection mechanisms under anaerobic conditions (Huang et al., 2020; Keiluweit et al., 2017). Microbes may use different carbon substrates under anaerobic and aerobic conditions, resulting in similar overall soil carbon decomposition (Huang et al., 2020). However, this trade-off may play minor roles due to similar neutral effects were observed in all three soils (which experience distinct land uses and have distinct soil properties, Table 1) and at all measurement times (Figure 5a).The

insignificant response of the decomposition of whole-soil carbon to soil core inversion may also imply that neither vertical substrate nor nutrient transport significantly alter whole-profile decomposition, or the 13-month incubation was too short to find a significant change in those transport (i.e., the absolute amount of transport is too small to take effect). Measurements of depth-specific O_2 availability and redistribution of dissolved components will help elucidate and disentangle their relative importance.

3.3 | Soil core inversion-induced soil respiration response to climate change

Depth relocation induced by soil core inversion also did not significantly influence the response of Rs to climate change, indicated by insignificant ($p > .05$) difference of slopes of the regression of Rs responses against elevation shifts between in non-inverted and in inverted soil cores (Figure 5b). It is intriguing to note that, at the first three measurement times (i.e., after 1, 4, and 7 months of field incubation), Rs did not significantly respond to elevation shifts ($p > .05$, Figure 5b). However, significant response manifested after 10 and 13 months of incubation ($p < .05$, Figure 5b). This result suggests that persistent SOC may be more sensitive to climate change (Davidson & Janssens, 2006; Karhu et al., 2010). Temperature could not explain such distinct temporal responses as temperature difference was consistently similar among the three elevations independent of measurement time (Figure 3), which may be due to exhaustion of labile SOC (Nottingham et al., 2019).

3.4 | Limitations and implications

An implicit assumption adopted by the inversion treatment is that the soil of same depth origin will experience different micro-environmental conditions when they are translocated to different soil depths. Although this assumption would be largely valid due to intact soil cores are incubated, we acknowledge that those soil properties of interest should be directly measured and/or monitored (in our case study, we did not separate Rs to different soil depths). In addition, the effects would need a long time to manifest and vary widely depending on edaphic properties of the incubated soil and climate conditions. This will be a challenge for field work. For example, in our case study, the 13-month incubation is still relatively short compared with the turnover time of SOM, which may range from centuries to millennia (Luo et al., 2019; Shi et al., 2020). As incubation proceeds, SOM may show different responses to depth relocation and climate shifts if the decomposer community adjusts its substrate utilization strategy and efficiency with the change of the quantity and quality of remaining SOM (Melillo et al., 2017). To allow multiple non-destructive sampling, more soil cores would need to be extracted and incubated if the interest is the long-term temporal dynamics.

SOM in deeper layers have slower turnover rates (or older ages) than that in upper layers (Shi et al., 2020; Xiao et al., 2022). The mechanism underpinning such phenomenon has been widely debated. Our case study suggests that vertical gradients of environmental conditions may play a minor role, at least for short-term whole-core SOM mineralization, albeit we did not directly measure depth-specific Rs. There must be some other profile gradients resulting in the apparent gradient of SOM persistence. The vertical distribution of the quantity and quality of carbon sources would be a dominant one. Topsoil SOM is mostly plant-derived, while subsoil SOM is microbial-derived (e.g., necromass, Ni et al., 2020) which is relatively small in terms of particle size and can be more effectively stabilized via physiochemical protection processes (He et al., 2021). Indeed, the ratio of POC to MOC is significantly larger in the topsoil than that in subsoil across the three elevations (Table 1). The alkyl C is usually derived from microbial metabolites and plant biopolymers and also increases with soil depth (Figure 4). In addition, microbial decomposition of subsoil SOM is usually nutrient-sufficient relative to decomposition in upper layers or in a nutrient-rich environment due to nutrient leaching (particularly nitrogen) from upper layers, resulting in energy limitation of subsoil SOM decomposition (Fontaine et al., 2007). Our data also showed that microbial C:N ratio (i.e., MBC:MBN) decreased with soil depth, and inorganic nitrogen per unit MBC increased with soil depth (Table 1), implying energy limitation in deeper layers. It will be very useful to assess depth-specific microbial community structure and activity as well as SOM composition as impacted by the inversion treatment when the incubation is long enough to detect SOM pool changes at different soil depths.

We have presented an innovative field incubation approach enabling non-destructive alteration of depth location of soil. Combining with a field translocation experiment, our case study provides in situ evidence that neither whole-soil SOM mineralization nor its response to climate change is significantly affected by the depth location of SOM, suggesting that depth-induced environmental gradients may be secondary. However, temporal measurements suggest that persistent SOC is more sensitive to climate change than labile SOC, implying that global subsoil would be also sensitive to climate change (Mao et al., 2022; Qin et al., 2019; Xu et al., 2021). Due to the neutral effect of profile environmental gradients, we suggest that depth-specific nature of carbon inputs and their microbial utilization and residues would be the driving force of the apparent gradient of SOM persistence through soil profile. Together with measurements/monitoring of vertical physiochemical conditions, the inversion experiment can provide an experimental initiating platform to elucidate the depth dependence of the response of soil biogeochemical processes to climate change and explore underlying mechanisms.

CONFLICT OF INTEREST

The authors declare no competing financial interests.

DATA AVAILABILITY STATEMENT

The data that support the findings of this study are available in Data Dryad at: https://doi.org/10.5061/dryad.18931zd0f.

ORCID

Xiaowei Guo https://orcid.org/0000-0002-5765-3438
Xiali Mao https://orcid.org/0000-0003-1084-8980
Liujun Xiao https://orcid.org/0000-0002-1900-1586
Mingming Wang https://orcid.org/0000-0002-1094-1029
Shuai Zhang https://orcid.org/0000-0003-0388-6989
Jinyang Zheng https://orcid.org/0000-0002-5282-9713
Hangxin Zhou https://orcid.org/0000-0002-2072-882X
Jinfeng Chang https://orcid.org/0000-0003-4463-7778
Zhou Shi https://orcid.org/0000-0003-3914-5402
Zhongkui Luo https://orcid.org/0000-0002-6744-6491

REFERENCES

Ahrens, B., Braakhekke, M. C., Guggenberger, G., Schrumpf, M., & Reichstein, M. (2015). Contribution of sorption, DOC transport and microbial interactions to the ^{14}C age of a soil organic carbon profile: Insights from a calibrated process model. *Soil Biology and Biochemistry*, *88*, 390–402.

Baldock, J. A., Oades, J. M., Nelson, P. N., Skene, T. M., Golchin, A., & Clarke, P. (1997). Assessing the extent of decomposition of natural organic materials using solid-state C-13 NMR spectroscopy. *Australian Journal of Soil Research*, *35*, 1061–1083.

Batjes, N. H. (2014). Total carbon and nitrogen in the soils of the world. *European Journal of Soil Science*, *65*, 10–21.

Bossio, D. A., & Scow, K. (1998). Impacts of carbon and flooding on soil microbial communities: Phospholipid fatty acid profiles and substrate utilization patterns. *Microbial Ecology*, *35*, 265–278.

Cotrufo, M. F., Ranalli, M. G., Haddix, M. L., Six, J., & Lugato, E. (2019). Soil carbon storage informed by particulate and mineral-associated organic matter. *Nature Geoscience*, *12*, 989–994.

Davidson, E. A., & Janssens, I. A. (2006). Temperature sensitivity of soil carbon decomposition and feedbacks to climate change. *Nature*, *440*(7081), 165–173.

Ebrahimi, A., & Or, D. (2016). Microbial community dynamics in soil aggregates shape biogeochemical gas fluxes from soil profiles–Upscaling an aggregate biophysical model. *Global Change Biology*, *22*(9), 3141–3156.

Efron, B., & Tibshirani, R. (1993). An introduction to the bootstrap. *Monographs on Statistics and Applied Probability*, *57*, 1–436.

Fontaine, S., Barot, S., Barré, P., Bdioui, N., Mary, B., & Rumpel, C. (2007). Stability of organic carbon in deep soil layers controlled by fresh carbon supply. *Nature*, *450*(7167), 277–280.

Friedlingstein, P., O'Sullivan, M., Jones, M. W., Andrew, R. M., Hauck, J., Olsen, A., Peters, G. P., Peters, W., Pongratz, J., Sitch, S., Le Quéré, C., Canadell, J. G., Ciais, P., Jackson, R. B., Alin, S., Aragão, L. E. O. C., Arneth, A., Arora, V., Bates, N. R., ... Zaehle, S. (2020). Global carbon budget 2020. *Earth System Science Data*, *12*(4), 3269–3340.

He, M., Fang, K., Chen, L., Feng, X., Qin, S., Kou, D., He, H., Liang, C., & Yang, Y. (2021). Depth-dependent drivers of soil microbial necromass carbon across Tibetan alpine grasslands. *Global Change Biology*, *28*(3), 936–949.

Hicks Pries, C. E., Castanha, C., Porras, R. C., & Torn, M. S. (2017). The whole-soil carbon flux in response to warming. *Science*, *355*(6332), 1420–1423.

Hu, Y., Jiang, L., Wang, S., Zhang, Z., Luo, C., Bao, X., Niu, H., Xu, G., Duan, J., Zhu, X., Cui, S., & Du, M. (2016). The temperature sensitivity of ecosystem respiration to climate change in an alpine meadow on the Tibet plateau: A reciprocal translocation experiment. *Agricultural and Forest Meteorology*, *216*, 93–104.

Huang, W., Ye, C., Hockaday, W. C., & Hall, S. J. (2020). Trade-offs in soil carbon protection mechanisms under aerobic and anaerobic conditions. *Global Change Biology*, *26*(6), 3726–3737.

Jobbágy, E. G., & Jackson, R. B. (2000). The vertical distribution of soil organic carbon and its relation to climate and vegetation. *Ecological Applications*, *10*(2), 423–436.

Karhu, K., Fritze, H., Tuomi, M., Vanhala, P., Spetz, P., Kitunen, V., & Liski, J. (2010). Temperature sensitivity of organic matter decomposition in two boreal forest soil profiles. *Soil Biology and Biochemistry*, *42*(1), 72–82.

Keiluweit, M., Wanzek, T., Kleber, M., Nico, P., & Fendorf, S. (2017). Anaerobic microsites have an unaccounted role in soil carbon stabilization. *Nature Communications*, *8*(1), 1771.

Kirschbaum, M. U. F., Don, A., Beare, M. H., Hedley, M. J., Pereira, R. C., Curtin, D., McNally, S. R., & Lawrence-Smith, E. J. (2021). Sequestration of soil carbon by burying it deeper within the profile: A theoretical exploration of three possible mechanisms. *Soil Biology and Biochemistry*, *163*, 108432.

Lehmann, J., & Kleber, M. (2015). The contentious nature of soil organic matter. *Nature*, *528*(7580), 60–68.

Li, J., Pei, J., Pendall, E., Reich, P. B., Noh, N. J., Li, B., Fang, C., & Nie, M. (2020). Rising temperature may trigger deep soil carbon loss across Forest ecosystems. *Advanced Science*, *7*(19), 2001242.

Luo, Z., Luo, Y., Wang, G., Xia, J., & Peng, C. (2020). Warming-induced global soil carbon loss attenuated by downward carbon movement. *Global Change Biology*, *26*(12), 7242–7254.

Luo, Z., Wang, G., & Wang, E. (2019). Global subsoil organic carbon turnover times dominantly controlled by soil properties rather than climate. *Nature Communications*, *10*(1), 3688.

Maier, M., & Schack-Kirchner, H. (2014). Using the gradient method to determine soil gas flux: A review. *Agricultural and Forest Meteorology*, *192-193*, 78–95.

Mao, X., Zheng, J., Yu, W., Guo, X., Xu, K., Zhao, R., Xiao, L., Wang, M., Jiang, Y., Zhang, S., Luo, L., Chang, J., Shi, Z., & Luo, Z. (2022). Climate-induced shifts in composition and protection regulate temperature sensitivity of carbon decomposition through soil profile. *Soil Biology and Biochemistry*, *172*, 108743.

Melillo, J. M., Frey, S. D., DeAngelis, K. M., Werner, W. J., Bernard, M. J., Bowles, F. P., Pold, G., Knorr, M. A., & Grandy, A. S. (2017). Long-term pattern and magnitude of soil carbon feedback to the climate system in a warming world. *Science*, *358*(6359), 101–105.

Ni, H., Jing, X., Xiao, X., Zhang, N., Wang, X., Sui, Y., Sun, B., & Liang, Y. (2021). Microbial metabolism and necromass mediated fertilization effect on soil organic carbon after long-term community incubation in different climates. *The ISME Journal*, *15*(9), 2561–2573.

Ni, X., Liao, S., Tan, S., Peng, Y., Wang, D., Yue, K., Wu, F., & Yang, Y. (2020). The vertical distribution and control of microbial necromass carbon in forest soils. *Global Ecology and Biogeography*, *29*(10), 1829–1839.

Nottingham, A. T., Whitaker, J., Ostle, N. J., Bardgett, R. D., McNamara, N. P., Fierer, N., Salinas, N., Ccahuana, A. J., Turner, B. L., & Meir, P. (2019). Microbial responses to warming enhance soil carbon loss following translocation across a tropical forest elevation gradient. *Ecology Letters*, *22*(11), 1889–1899.

Preusser, S., Marhan, S., Poll, C., & Kandeler, E. (2017). Microbial community response to changes in substrate availability and habitat conditions in a reciprocal subsoil transfer experiment. *Soil Biology and Biochemistry*, *105*, 138–152.

Qin, S., Chen, L., Fang, K., Zhang, Q., Wang, J., Liu, F., Yu, J., & Yang, Y. (2019). Temperature sensitivity of SOM decomposition governed

by aggregate protection and microbial communities. *Science Advances*, 5(7), eaau1218.

R Core Team. (2022). *R: A language and environment for statistical computing*. R Foundation for Statistical Computing. https://www.R-project.org/

Rumpel, C., & Kögel-Knabner, I. (2011). Deep soil organic matter—A key but poorly understood component of terrestrial C cycle. *Plant and Soil*, 338(1), 143–158.

Salomé, C., Nunan, N., Pouteau, V., Lerch, T. Z., & Chenu, C. (2010). Carbon dynamics in topsoil and in subsoil may be controlled by different regulatory mechanisms. *Global Change Biology*, 16(1), 416–426.

Schmidt, M. W., Torn, M. S., Abiven, S., Dittmar, T., Guggenberger, G., Janssens, I. A., Kleber, M., Kögel-Knabner, I., Lehmann, J., Manning, D. A., Nannipieri, P., Rasse, D. P., Weiner, S., & Trumbore, S. E. (2011). Persistence of soil organic matter as an ecosystem property. *Nature*, 478(7367), 49–56.

Shi, Z., Allison, S. D., He, Y., Levine, P. A., Hoyt, A. M., Beem-Miller, J., Zhu, Q., Wieder, W. R., Trumbore, S., & Randerson, J. T. (2020). The age distribution of global soil carbon inferred from radiocarbon measurements. *Nature Geoscience*, 13(8), 555–559.

Sokol, N. W., Slessarev, E., Marschmann, G. L., Nicolas, A., Blazewicz, S. J., Brodie, E. L., Firestone, M. K., Foley, M. M., Hestrin, R., Hungate, B. A., Koch, B. J., Stone, B. W., Sullivan, M. B., Zablocki, O., LLNL Soil Microbiome Consortium, & Pett-Ridge, J. (2022). Life and death in the soil microbiome: How ecological processes influence biogeochemistry. *Nature Reviews Microbiology*, 20(7), 415–430.

Vance, E., Brookes, P., & Jenkinson, D. (1987). An extraction method for measuring soil microbial biomass C. *Soil Biology and Biochemistry*, 19, 703–707.

Vaughn, L. J., & Torn, M. S. (2019). [14] C evidence that millennial and fast-cycling soil carbon are equally sensitive to warming. *Nature Climate Change*, 9(6), 467–471.

Xiao, L., Wang, G., Wang, M., Zhang, S., Sierra, C. A., Guo, X., Chang, J., Shi, Z., & Luo, Z. (2022). Younger carbon dominates global soil carbon efflux. *Global Change Biology*, 25(18), 5587–5599.

Xu, M., Li, X., Kuyper, T. W., Xu, M., Li, X., & Zhang, J. (2021). High microbial diversity stabilizes the responses of soil organic carbon decomposition to warming in the subsoil on the Tibetan Plateau. *Global Change Biology*, 27(10), 2061–2075.

Zimmermann, M., Meir, P., Bird, M. I., Malhi, Y., & Ccahuana, A. (2009). Climate dependence of heterotrophic soil respiration from a soil-translocation experiment along a 3000 m tropical forest altitudinal gradient. *European Journal of Soil Science*, 60(6), 895–906.

SUPPORTING INFORMATION

Additional supporting information can be found online in the Supporting Information section at the end of this article.